Manganese porphyrin-containing polymeric micelles: A novel approach for intracellular catalytic formation of per/polysulfide species from a hydrogen sulfide donor

Kemper Young, Setsuko Yamane, Elmira Abbasi Ghareh Tapeh, Shingo Kasamatsu, Hideshi Ihara, Urara Hasegawa\*

K. Young, S. Yamane, E.A. Ghareh Tapeh, U. Hasegawa

Department of Materials Science and Engineering, The Pennsylvania State University, Steidle Building, University Park, PA 1680, USA

E-mail: uph5002@psu.edu

#### S. Yamane

Department of Chemistry & Biochemistry, National Institute of Technology, Numazu College 3600 Ooka, Numazu, Shizuoka 410-8501, Japan

S. Kasamatsu, H. Ihara

Department of Biological Chemistry, Osaka Metropolitan University, 1-1 Gakuen-cho, Sakai, Osaka 599-8531, Japan

Keywords: Polysulfides, Hydrogen sulfide, Manganese porphyrin, Polymeric micelles, Angiogenesis

#### **Abstract**

Per/polysulfide species that are generated from endogenously produced hydrogen sulfide have critical regulatory roles in a wide range of cellular processes. However, the lack of delivery systems that enable controlled and sustained release of these unstable species in biological systems hinders the advancement of sulfide biology research as well as translation of knowledge to therapeutic applications. Here, we developed a novel approach to generate per/polysulfide species in cells by combining a H<sub>2</sub>S donor and manganese porphyrincontaining polymeric micelles (MnPMCs) that catalyze oxidization of H<sub>2</sub>S to per/polysulfide species. MnPMCs served as a catalyst for H<sub>2</sub>S oxidation in aerobic phosphate buffer. HPLC-MS/MS analysis revealed that H<sub>2</sub>S oxidation by MnPMCs in the presence of glutathione results in the formation of glutathione-S<sub>n</sub>H (n=2 and 3). Furthermore, co-treatment of human

umbilical vein endothelial cells (HUVECs) with the H<sub>2</sub>S donor anethole dithiolethione and MnPMCs increased intracellular per/polysulfide levels and induced a proangiogenic response. Co-delivery of MnPMCs and a H<sub>2</sub>S donor is a promising approach for controlled delivery of polysulfides for therapeutic applications.

#### 1. Introduction

Hydrogen sulfide (H<sub>2</sub>S) and related sulfur species have emerged as essential signal mediators that regulate many cellular processes in the human body. After the pioneering work of the potential neuromodulatory roles of endogenous H<sub>2</sub>S in 1996, [1] its biological functions in different cells and tissues have been extensively studied. Those studies have shown that H<sub>2</sub>S is involved in signal transduction in the cardiovascular, [2] nervous[3] and immune systems, [4] as well as cancer. [5] Further mechanistic investigations revealed that the majority of the reported activities is attributed to post-translational modification of target proteins via Ssulfhydration of cysteine residues (i.e., cysteine-SSH).<sup>[6]</sup> However, given its relatively low reactivity, it is unlikely that H<sub>2</sub>S (or HS<sup>-</sup>) can directly modify cysteine-SH under physiological conditions.<sup>[7]</sup> Since H<sub>2</sub>S is catabolized to more reactive sulfur species via sulfide oxidation pathways, it has been hypothesized that the actual signal mediators could be the downstream products of H<sub>2</sub>S. Among the possible sulfur species, hydroper/polysulfides (RS<sub>n</sub>H, n>2), polysulfides (RS<sub>n+1</sub>R, n>2) and hydrogen per/polysulfide ( $H_2S_n$ , n>2) (hereafter referred to as "polysulfides") have attracted attention due to their high nucleophilicity. Accumulating evidence suggests that many biological activities that were originally attributed to H<sub>2</sub>S are likely to be due to polysulfide species.<sup>[8]</sup>

With a growing interest in the biological significance of polysulfides, there is a need for development of administration technologies that mimic the continuous polysulfide generation in the body in order to advance understanding of sulfide biology as well as explore their potential therapeutic applications. Because polysulfides are inherently unstable and readily

decompose, it is challenging to deliver these species to target cells or tissues in a controlled manner. Thus far, several persulfide donor molecules that generate hydropersulfides have been reported. Examples include cyclic acyl disulfides,<sup>[9]</sup> persulfides caged with ohydroxydihydrocinnamic acid derivatives,<sup>[10]</sup> *N*-acetyl cysteine persulfides with H<sub>2</sub>O<sub>2</sub>- and enzyme-sensitive protecting groups,<sup>[11]</sup> and protected perthiocarbonates.<sup>[12]</sup> However, most persulfide donors show relatively fast release profiles and controlling persulfide release rates remains a challenge. Apart from those persulfide donors, recent studies show that superoxide dismutase (SOD) as well as manganese porphyrin complexes (SOD mimetics) can catalyze the formation of polysulfide species from H<sub>2</sub>S in aerobic buffers.<sup>[13]</sup> In addition, it is also reported that the conversion of H<sub>2</sub>S to polysulfides can be catalyzed by myoglobin.<sup>[14]</sup> Given that a wide variety of H<sub>2</sub>S donors with sustained or stimuli-sensitive release profiles is available due to the extensive research on H<sub>2</sub>S donors in the past decade,<sup>[15]</sup> it is expected that the combination of such H<sub>2</sub>S donors with H<sub>2</sub>S oxidizing catalysts can be an alternative approach that enables controlled generation of polysulfide species in biological systems for achieving desired therapeutic outcomes.

Here, we report a novel polysulfide delivery system using polymeric nanocatalyst in combination with a H<sub>2</sub>S donor. Intracellular polysulfide formation is achieved by the catalytic oxidation of H<sub>2</sub>S released from H<sub>2</sub>S donors. We synthesized polymeric micelles containing manganese porphyrin (MnPMCs) as the H<sub>2</sub>S oxidation catalyst, and investigated its catalytic activity to generate polysulfide species from H<sub>2</sub>S in physiological buffer. We also observed that the micelles catalyze the conversion of H<sub>2</sub>S, which is released from the H<sub>2</sub>S donor anethole dithiolone (ADT), to polysulfide species in human umbilical vein endothelial cells (HUVECs). Furthermore, the proangiogenic effect of the co-treatment with MnPMCs and ADT was evaluated in HUVECs.

#### 2. Results and Discussion

#### 2.1. Preparation of manganese porphyrin-containing micelle

The design concept of manganese-porphyrin containing-micelles (MnPMC) is outlined in **Figure 1**. We first synthesized an amphiphilic diblock copolymer consisting of hydrophilic poly(acryloyl morpholine) (PAM) and hydrophobic and amine-reactive poly(pentafluorophenyl acrylate) (PPFPA) segments. [16] This diblock copolymer was used to prepare micelles in water. The pentafluorophenyl (PFP) ester groups within the micelle core were reacted with porphyrin bearing four amino groups (porphyrin amine) [17] to yield porphyrin-conjugated micelles (PMC). Then, PMCs were complexed with manganese to obtain MnPMC that catalyze the oxidation of H<sub>2</sub>S to polysulfides.

The PAM-PPFPA block copolymer was synthesized via RAFT polymerization as previously reported (**Scheme S1**). [16] 1H NMR showed the composition to be PAM<sub>92</sub>-PPFPA<sub>26</sub> and SEC-MALLS showed the polymer to have a M<sub>w</sub>/M<sub>n</sub> value of 1.02 (**Table S1**, **Figure S1** and **S2**). To synthesize porphyrin-conjugated micelles (PMC), the PAM-PPFPA polymer was dissolved in dimethyl formamide and added to an aqueous solution of porphyrin amine under stirring. As shown in **Scheme 1a**, the amino groups of porphyrin amine were reacted with PFP ester groups, resulting in the formation of crosslinked micelles. Thereafter, the remaining PFP ester groups were reacted with excess benzylamine followed by purification (ultrafiltration and dialysis).

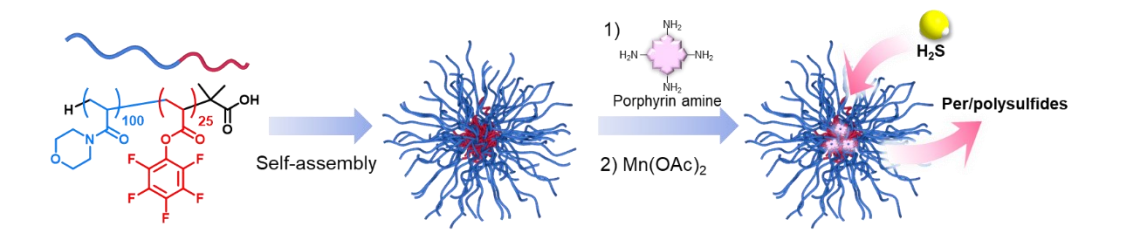
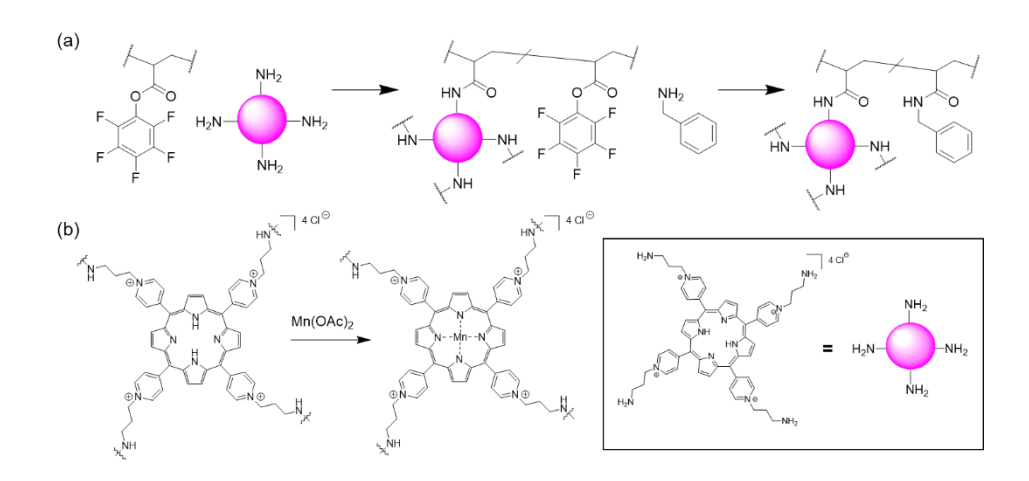


**Figure 1.** Manganese porphyrin-containing micelles (MnPMCs) for catalytic formation of polysulfides. MnPMCs were prepared by conjugating porphyrin amine to the pentafluorophenyl groups of the PAM-PPFPA micelles followed by complexation with manganese.



**Scheme 1.** Preparation of MnPMCs. (a) Conjugation of porphyrin amine to the micellar core via reaction with the pentafluorophenyl ester groups. (b) Chemical structure of porphyrin amine. (c) Complexation of PMC with Mn(OAc)<sub>2</sub> to form MnPMC.

As shown in **Table 1**, different porphyrin/PFPA molar feed ratios were used to synthesize PMCs. Notably, feed ratios of 0.025 and 0.05 (PMC1 and 2) led to near quantitative incorporation of the added porphyrin amine whereas a higher feed ratio of 0.1 led only to 57% incorporation (PMC3). This suggests that porphyrin amine mainly reacted with PFP ester groups close to the surface of the micellar core. In light of porphyrin amine's high aqueous solubility, it is not surprising that porphyrin amine favors the aqueous phase rather than the hydrophobic micellar core. The presence of porphyrin on the surface of the micellar core facing the aqueous phase will be beneficial since it can readily interact with H<sub>2</sub>S/HS<sup>-</sup> in solution and catalyze its oxidation to polysulfides.

**Table 1.** Characterization of porphyrin-conjugated micelles (PMCs).

Sample	Molar feed ratio [Porphyrin]/ [PFPA]	% Reaction <sup>a)</sup>	$N_{porph}^{b)}$	D <sub>h</sub> [nm] <sup>c)</sup>	PDI <sup>d)</sup>
PMC1	0.025	97	0.61	34.0	0.33
PMC2	0.05	94	1.17	38.4	0.26
PMC3	0.1	57	1.42	36.8	0.35

a) Absorbance at 425 nm of the filtrate obtained after ultrafiltration was measured to determine the amount of unreacted porphyrin (**Figure S3**), which was used to calculate % reaction; b) Number of porphyrin groups per polymer as calculated from % reaction and the

feed ratio; c) Hydrodynamic diameter (Z-average) and polydispersity index (PDI) as measured by DLS using the cumulant method.

PMCs were reacted with manganese acetate (Mn(OAc)<sub>2</sub>) at 40°C to complex the porphyrin with the Mn cation. We first measured UV-Vis spectra of porphyrin amine after the reaction with different amounts of Mn(OAc)<sub>2</sub> as shown in Figure S4. The Soret band of porphyrin amine, which appears at 425 nm, shifts to 464 nm showing an isosbestic point of 450 nm upon Mn complexation. The spectral change was no longer observed when the amount of Mn(OAc)<sub>2</sub> was above 100 equivalent relative to porphyrin amine, indicating complete Mn complexation. We next reacted PMCs with Mn(OAc)<sub>2</sub> at different molar ratios. Based on the spectra obtained with Mn-porphyrin amine, we determined the degree of Mn complexation for the reaction between PMCs and Mn(OAc)<sub>2</sub> as shown in Figure 2a and Figure S5. The degree of complexation was nearly quantitative (above 90%) for PMC1 and 2 after the addition of 10 and 50 equivalent of Mn(OAc)2, respectively (Table 2). On the other hand, PMC3 showed a significantly lower degree of complexation of 76% even after the addition of 200 equivalent of Mn(OAc)<sub>2</sub>. While the reason for this different reactivity of porphyrin in micelles is not clear, it is possible that the local environment of porphyrin, such as hydrophobicity and the presence of unreacted amine groups of porphyrin and carboxyl group due to hydrolysis of PFP ester, affects the metalation reaction. Furthermore, the absence of PFPA group or pentafluorophenol (hydrolysis product) was confirmed by <sup>19</sup>F NMR (**Figure S6**).

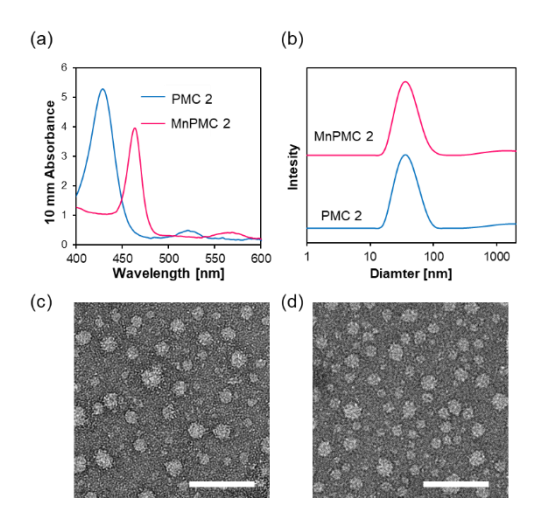


**Figure 2.** Characterization of MnPMC. (a) UV-Vis spectra of PMC2 before and after Mn complexation. PMC2 was incubated with 10 eq. Mn(OAc)<sub>2</sub> in water for 24 h at 37°C. (b) Size distribution of PMC2 and MnPMC2 by DLS. (c,d) TEM images of (c) PMC2 and (d) MnPMC2 stained with 2wt% uranyl acetate solution. Scale bars: 100 nm.

Dynamic light scattering (DLS) was performed to determine the size distribution of PMCs and MnPMCs. As can be seen in **Figure 2b**, **Table 1** and **2**, the average diameters of the micelles were in the range of 34-40 nm with relatively narrow size distribution. In addition, Mn complexation did not lead to dramatic changes in size distribution. Furthermore, the spherical morphology of PMC2 and MnPMC2 was observed by TEM after staining negatively with uranyl acetate as shown in **Figure 2c** and **d**.

**Table 2.** % Mn complexation by PMC and size distributions of the MnPMCs.

Sample	% Mn complexation <sup>a)</sup>	D <sub>h</sub> [nm] <sup>b)</sup>	PDI <sup>b)</sup>
MnPMC1	93	37.2	0.23
MnPMC2	92	39.3	0.27
MnPMC3	76	40.0	0.28

a) Determined by UV-Vis spectroscopy (see experimental); b) Hydrodynamic diameter (Z-average) and polydispersity index (PDI) as measured by DLS using the cumulant method.

#### 2.2. Stability of MnPMCs in the presence of serum proteins

The stability of MnPMCs was investigated in the presence of serum proteins. It is known that porphyrins often aggregate in biological media or adsorb to serum proteins such as albumin. Such effects can be characterized by a decreased extinction coefficient and broader Soret and Q bands of the porphyrin ring. We incubated MnPMCs with fetal bovine serum (FBS) at 37°C and measured UV-Vis spectra over the course of two days. As shown in **Figure 3**, both Mn-porphyrin amine and MnPMC3 led to a significant decrease of the absorbance of the Soret (460 nm) and Q (570 nm) bands, whereas no significant spectral change was observed for MnPMC1 and MnPMC2. This might be due to the unreacted amino group in MnPMC3, which facilitates the interaction between porphyrin and serum protein. For further investigation, MnPMC2 was used to characterize its catalytic activity for polysulfide formation due to its high stability in the presence of serum and high porphyrin content.

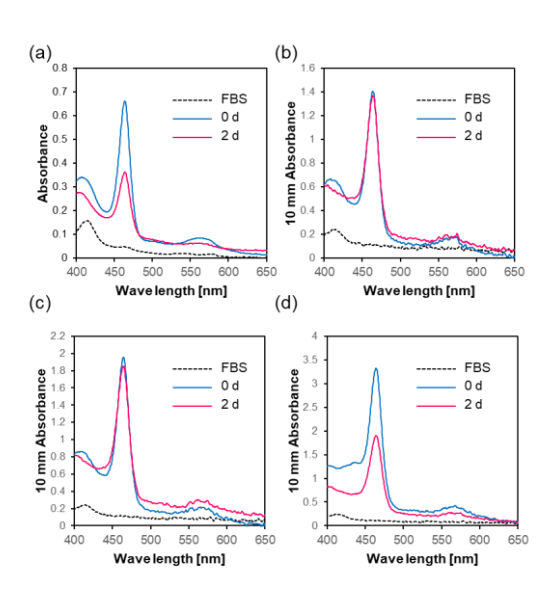


**Figure 3.** Stability of MnPMCs. UV-Vis spectra of (a) Mn-porphyrin amine, (b) MnPMC1 (c) MnPMC2 and (d) MnPMC3 incubated in 10% FBS at 37°C for 2 d. The spectra were collected using (a) a cuvette with 10 mm light path or (b-d) the pedestal mode of Nanodrop. Blue: 0 d, Pink: 2 d, Black: FBS alone.

#### 2.3. Catalytic activity of MnPMCs to convert H2S to polysulfides

It has been reported that a series of Mn-porphyrin complexes can catalyze oxidation of  $H_2S$  in the presence of oxygen. According to the mechanism proposed by Olson et al., the hydrosulfide anion ( $HS^-$ ) is oxidized by Mn(III), resulting in the formation of hydrosulfide radicals ( $HS^{\bullet}$ ) and then hydrogen persulfide ( $H_2S_2$ ).<sup>[13a]</sup> Mn(II) will then be oxidized by oxygen to regenerate Mn(III). Furthermore, the  $HS_2^-$  anion can be further oxidized by Mn(III) and form higher order polysulfides ( $H_2S_n$  (n>2)).

Here, the catalytic activity of MnPMCs to convert  $H_2S$  to polysulfide species was investigated in phosphate buffer saline (PBS). In this experiment, we used sodium sulfide (Na<sub>2</sub>S, sodium salt of  $H_2S$ ) as the  $H_2S$  donor, which generates  $H_2S/HS^-$  instantaneously in physiological buffers.<sup>[19]</sup> To detect the formation of polysulfides, we used the SSP4 fluorescent sulfane sulfur detection dye.<sup>[20]</sup> As shown in **Figure 4a**, the mixing of MnPMC2 with Na<sub>2</sub>S led to a gradual increase of fluorescence over the course of 2 h. Importantly, PMC2, which was not complexed with Mn cation, did not show this increase while the fluorescence intensity was slightly higher than that of the control containing Na<sub>2</sub>S and SSP4. These results shows that the Mn-porphyrin complex in MnPMC2 is catalytically active and capable of oxidizing  $H_2S$  to  $H_2S_n$  (n>2).

To further investigate the catalytic activity of MnPMC2 to form polysulfides from H<sub>2</sub>S, we used a HPLC-MS/MS method with *N*-iodoacetyl L-tyrosine methyl ester (TME-IAM) as the trapping reagent.<sup>[21]</sup> In this assay, TME-IAM is used to form stable adducts with polysulfides that can be analyzed by HPLC-MS/MS. Here, we reacted MnPMC2, Na<sub>2</sub>S and glutathione to generate glutathione polysulfides (GS<sub>n</sub>H, n>2), which were trapped by TME-IAM (**Figure 4b**). To determine the retention time of the GS<sub>n</sub>-TME-IAM adducts, we first reacted glutathione with sodium persulfide (Na<sub>2</sub>S<sub>2</sub>) and measured the mixture of different adducts by HPLC-MS/MS. Under the condition as described in the experimental section, we identified

three glutathione adducts based on their M+H masses at 543 (n =1), 575 (n=2) and 607 (n=3). We then used this HPLC-MS/MS method to analyze polysuffides that were generated by mixing MnPMC2, Na<sub>2</sub>S and glutathione. As shown in **Figure 4c**, only MnPMC2 showed the formation of the n=2 adduct (73%). In addition, a small amount of the n=3 adduct could be detected for MnPMC2 (1%), which was absent for PMC2 and water. The small amounts of the n=2 adducts observed for PMC2 (7%) and water (NT) (3%) are probably due to the noncatalytic oxidation of H<sub>2</sub>S by air. Formation of GS<sub>n</sub>H adducts is likely to form via a three-step process: oxidation of H<sub>2</sub>S to H<sub>2</sub>S<sub>n</sub> followed by reaction of H<sub>2</sub>S<sub>n</sub> with glutathione, which will be trapped by TME-IAM. During this process, it is also possible that H<sub>2</sub>S<sub>n</sub> forms the bis adducts with TME-IAM (S<sub>n</sub>-bis). Indeed, the XIC chromatograms showed m/z peaks for M+H<sup>+</sup> at 505, 537 and 569 corresponding to the n=1, 2 and 3 bis adducts, respectively. Only MnPMC2 showed a strong signal for n=2 (30%), whereas those for PMC (3%) and the control were much lower (2%) (**Figure 4d**). In the case of MnPMC2, a small amount (0.4%) of the n=3 adduct was also detected. Taken together these results clearly show that MnPMC2 catalyzed generation of H<sub>2</sub>S<sub>n</sub> (n>2), resulting in the formation of GS<sub>n</sub>H species.

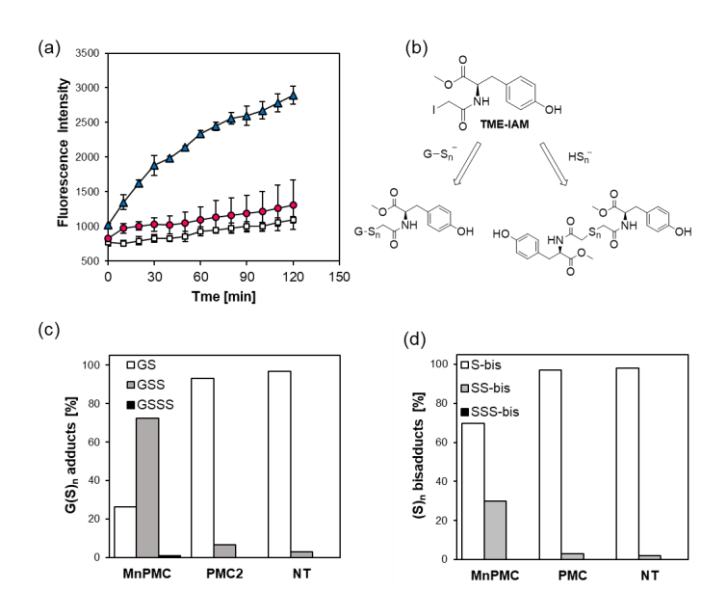


**Figure 4.** Catalytic activity of MnPMC to convert H<sub>2</sub>S to per/polysulfides. (a) Sulfane sulfur formation as function of time. MnPMC2 (triangle), PMC2 (circle) and water (square) were mixed with the SSP4 sulfane sulfur detection dye in PBS, and incubated at 37°C after adding

an aqueous Na<sub>2</sub>S solution. Fluorescence intensity ( $\lambda_{ex}$ =430-495 nm,  $\lambda_{em}$ =510-580 nm) was measured using an Invitrogen Qubit 4 fluorometer at different time points. Porphyrin: 2  $\mu$ M, SSP4: 10  $\mu$ M Na<sub>2</sub>S: 100  $\mu$ M. n=3. (b) Reaction between TME-IAM and polysulfides. G: Glutathione. (c, d) Per/polysulfide species as determined by HPLC-MS/MS using the TME-IAM trapping probe for per/polysulfide species. Glutathione and Na<sub>2</sub>S were reacted in the presence of MnPMC2 at pH 7.4 at 37°C for 2 h before adding a TME-IAE solution in DMSO. After ultrafiltration to remove MnPMC2 and PMC2 the filtrate was analyzed by HPLC-MS/MS.

# 2.4. Polysulfide formation in HUVECs treated with MnPMCs and the H<sub>2</sub>S donor anethole dithiolethione

Having shown the catalytic activity of MnPMC2 to generate polysulfides, we next investigated whether the micelles in combination with an exogenous H<sub>2</sub>S source are capable of increasing polysulfide levels in human umbilical vein endothelial cells (HUVECs). As the exogeneous H<sub>2</sub>S source, we used anethole dithiolone (ADT), a compound that is known to generate H<sub>2</sub>S upon oxidation by intracellular enzymes such as cytochromes P450 monooxygenase.<sup>[15i]</sup> To demonstrate that MnPMCs can catalyze polysulfide formation by oxidizing intracellular H<sub>2</sub>S, we used ADT as the H<sub>2</sub>S donor since it releases H<sub>2</sub>S within cells but not in the extracellular space.<sup>[15f]</sup>

HUVECs were preloaded with the SSP4 dye and treated with different formulations for 1.5 h. As shown in **Figure 5d**, HUVECs treated with ADT and MnPMC2 showed bright fluorescence indicating intracellular polysulfide formation. MnPMC2 alone did not show an obvious increase in fluorescence (**Figure 5c**). Furthermore, HUVECs treated with ADT alone showed weak fluorescence, which might be due to the natural sulfide oxidation mechanisms that exist in this cell line. These results clearly show that MnPMCs have catalytic activity to form polysulfide from intracellular H<sub>2</sub>S in HUVECs.

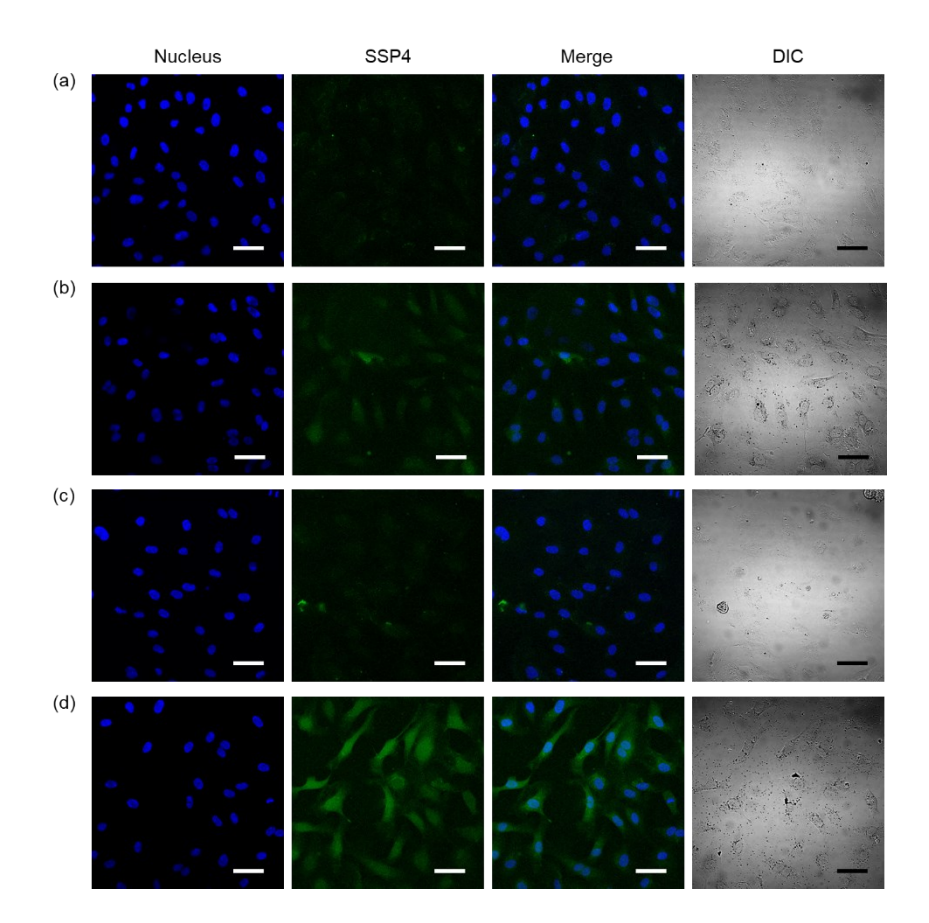


**Figure 5.** Sulfane sulfur formation in HUVECs. Cells were preloaded with the SSP4 sulfane sulfur detection dye and cultured for 1.5 h and observed by CLSFM. (a) medium alone (NT), (b) ADT, (c) MnPMC2 (d) MnPMC2 and ADT. MnPMC2: 2  $\mu$ M (Mn porphyrin), ADT 100  $\mu$ M. Blue: Nucleus (Hoechst 33342), Green: Per/polysulfide species (SSP4). Scale bars: 50  $\mu$ m.

#### 2.5. Proangiogenic activity of the polysulfide delivery system

Cellular production of H<sub>2</sub>S and related sulfane sulfur compounds is of particular importance for the vascular system. It has been reported that those sulfur species stimulate angiogenesis, enhance vascular permeability, and induce endothelial cell proliferation and migration. [15e, 22] Importantly, the majority of the reported activities are attributed to sulfhydration of cysteine residues of target proteins. [23] For example, persulfidation of the vascular endothelial growth factor receptor (VEGFR2), the receptor that binds the pro-angiogenic VEGF signal protein, leads to dimerization, phosphorylation and activation in endothelial cells. Angiogenesis is also induced through the activation of ATP-sensitive potassium channel via S-sulfhydration. [24] It should be noted that unlike H<sub>2</sub>S, polysulfide species are capable of sulfhydrating cysteine

residues directly.<sup>[7]</sup> Therefore, polysulfides are expected to serve as stronger regulators of endothelial functions compared to H<sub>2</sub>S.

We evaluated the proangiogenic effect of MnPMC2 and ADT in the HUVEC tube formation assay. In this assay, HUVECs seeded on a fibrin gel were treated with different formulations. As shown in **Figures 6** and **S7**, the combination of MnPMC2 and ADT induced tube formation, which is characterized by loop formation as a result of cell migration and alignment. In addition, filopodia were observed at tip cell fronts. On the other hand, only a weak tubulogenic effect was observed for ADT alone. Furthermore, MnPMC2 alone did not show any obvious effects on the HUVEC monolayer structure. These results clearly show that the conversion of H<sub>2</sub>S to polysulfides is required for stimulating endothelial cells tube formation. Furthermore, MnPMCs did not show obvious toxicity as determined by MTT assay (**Figure S8**).

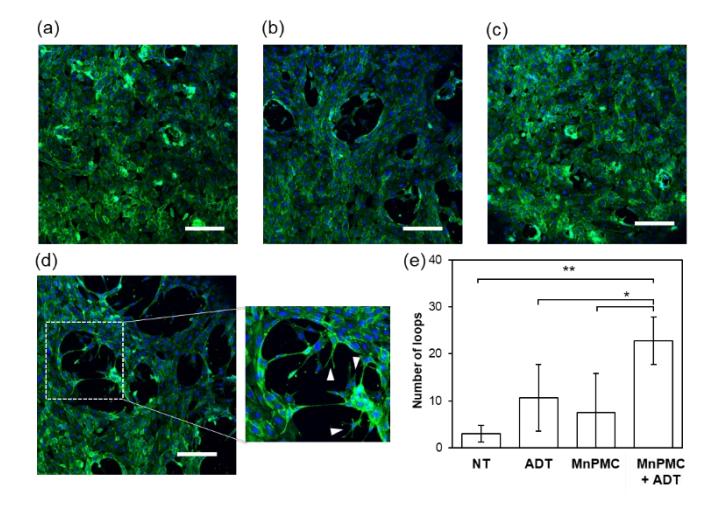


**Figure 6.** Proangiogenic activity in the HUVEC tube formation assay. Cells were seeded on fibrin gel-coated μ slide angiogenesis (ibidi) and cultured for 2 days. (a-d) CLSFM images of HUVECs cultured in the presence of (a) medium alone (NT), (b) ADT, (c) MnPMC2 and (d) MnPMC2 and ADT. MnPMC2: 5.8 μM (Mn porphyrin), ADT 10 μM. Cells were fixed, stained and observed by CLSFM. Green: Actin, Blue: nucleus. 2D compression of Z-stack images. Arrow heads indicate filopodia. Scale bars: 250 μm (e) Number of loops per well was determined from phase contrast microscopic images (**Figure S6**). \*p<0.05, \*\*p<0.01, n=3.

To get more insight into the effect of co-treatment with MnPMCs and ADT, cell elongation, cell alignment as well as changes in VE-cadherin and actin patterns of HUVECs were analyzed. In the angiogenesis process, endothelial cells are known to transform from a polygonal to elongated form.<sup>[25]</sup> Also, cells need to align and reshape to form the innermost layer of the blood vessel that acts as a barrier to confine blood within the vessel. One key player is VE-cadherin, which is responsible for cell-cell interactions.<sup>[26]</sup> It is known that cell junction dynamics and cell motility are enhanced during angiogenesis, which is characterized by an interrupted VE-cadherin pattern.<sup>[27]</sup> Furthermore, the enhanced actin stress fiber formation has a central role in cell migration. [28] In this experiment, a confluent monolayer of HUVECs cultured in a glass-based dish was treated with different formulations for 1 day. As shown in Figure 7d, the combination of MnPMC2 and ADT has a dramatic effect on cell shape leading to cell elongation and alignment. Also, polarized stress fiber formation as well as a partially interrupted VE-cadherin pattern were observed. It has been reported that VEGFR2, which is known to be activated via sulfhydration, is involved in regulation of cell alignment and polarity.<sup>[27]</sup> Actin mobility and the formation of stress fibers has also been observed for VEGFR2-mediated VEGF signaling.<sup>[8]</sup> In addition, a recent study reported the effect of polysulfide donor to mobilize cell junctions and induce stress fiber formation. [29] Therefore, the observed changes are likely to be due to polysulfide species, which were generated via oxidation of ADT-derived H<sub>2</sub>S by MnPMC2. As shown in Figure 7b, cell elongation was also observed in cells treated with ADT (H<sub>2</sub>S alone). However, the image analysis revealed that the cell elongation effect was much weaker than that of the combination of ADT and MnPMC2 (Figure S9). In addition, alignment analysis showed that the cell main axis was randomly distributed after treatment of ADT alone whereas enhanced cell alignment was observed in cells treated with ADT and MnPMC2 (Figure S10). These results are in agreement with our observation that the combination of ADT and MnPMC2 shows a much

stronger tubulogenic effect compared to ADT alone (**Figure 6**). Furthermore, it should be noted that MnPMC2 alone did not induce any obvious changes in cell morphology as well as VE-cadherin and actin patterns. Taken together, controlled intracellular delivery of polysulfide species was achieved by co-treatment of MnPMCs with the H<sub>2</sub>S donor ADT, demonstrating the importance of polysulfide species in stimulating angiogenesis in endothelial cells. The approach to use the combination of MnPMC-based nanocatalyst and a H<sub>2</sub>S donor can be applied for therapeutic delivery of polysulfides for facilitating wound healing and tissue repair.

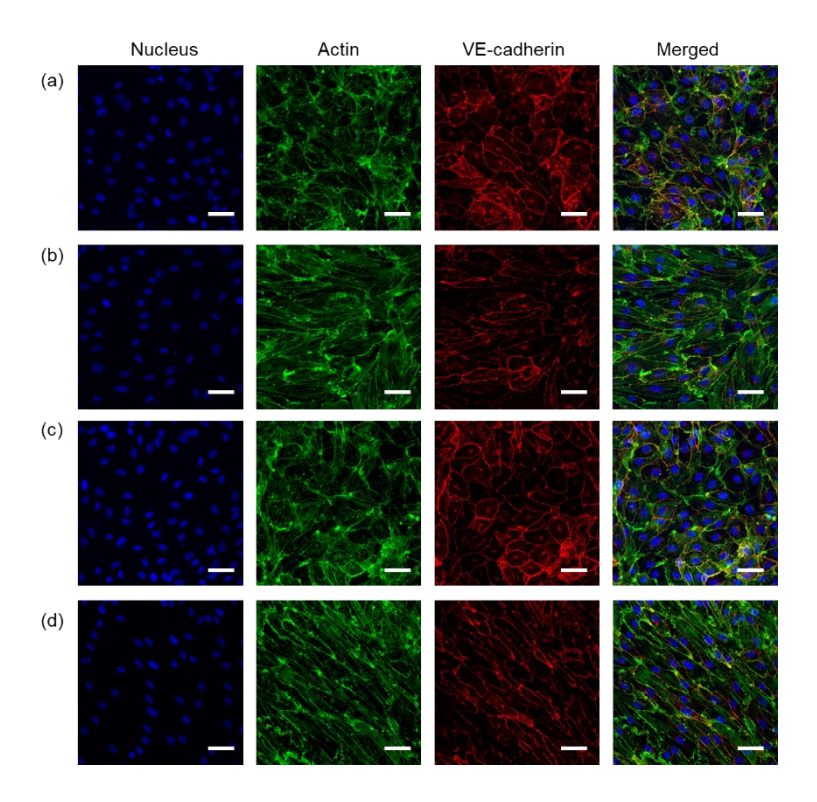


**Figure 7.** Changes in VE-cadherin and actin patterns in HUVECs. A confluent HUVEC monolayer was cultured in the presence of (a) medium alone (NT), (b) ADT, (c) MnPMC2 and (d) MnPMC2 and ADT for 1 day. MnPMC2: 5.8 μM (Mn porphyrin), ADT 10 μM. Cells were fixed, stained and observed by CLSFM. Green: Actin, Red: VE-cadherin, Blue: nucleus. 2D compression of Z-stack images. Scale bars: 50 μm.

#### 3. Conclusion

We developed a novel approach for intracellular delivery of polysulfide species by combining a H<sub>2</sub>S donor and polymeric micelles containing manganese porphyrin (MnPMC) that serve as

a catalyst to oxidize H<sub>2</sub>S to polysulfide species. MnPMCs catalyzed oxidation of H<sub>2</sub>S in aerobic buffer solution. MnPMCs in combination with a H<sub>2</sub>S donor anethole dithiolone (ADT) leads to an increase of intracellular polysulfide species in HUVECs. Furthermore, cotreatment with MnPMCs and ADT leads to enhanced proangiogenic response in HUVECs compared to ADT alone. Thus, this novel approach can be used to enhance the therapeutic effects of existing H<sub>2</sub>S donors by facilitating the formation of reactive polysulfides upon H<sub>2</sub>S release. Another advantage is that MnPMCs mimic enzymatic H<sub>2</sub>S oxidation in the human body, which is expected to be suited for controlled generation of polysulfides at physiologically relevant levels. The developed polysulfide delivery system based on MnPMC and the H<sub>2</sub>S donor will have potential for treatment of diseases requiring *S*-sulfhydration of proteins.

#### 4. Experimental Section/Methods

Synthesis of porphyrin-conjugated micelles (PMC): Porphyrin-conjugated micelles (PMC) were prepared by reacting porphyrin amine at different concentrations with PAM<sub>92</sub>-PPFPA<sub>26</sub> polymeric micelles. For preparing PMC1, 2 and 3, the porphyrin solutions were prepared by diluting 10.5, 21 and 42 μL of a 7.4 mM porphyrin amine solution with 500 μL water. Then, 25 μL of a 100 mg/mL PAM<sub>92</sub>-PPFPA<sub>26</sub>/DMF solution was added dropwise to the porphyrin solutions under vigorous stirring. After closing the glass vials, the reaction mixtures were stirred at 50°C to conjugate porphyrin. After 30 min, 13.6 μL of a 10 vol% benzylamine/DMF solution was added to the reaction mixture (benzylamine to PFPA group molar ratio of 4). After stirring at 50°C for 24 hours, the reaction mixtures were cooled down. The solutions were transferred to an Amicon ultrafiltration unit (MWCO 30 kDa) and centrifuged at 14,000 x g for 10 min. The filtrate was collected and measured by UV-Vis to quantify the amount of unreacted porphyrin amine. The sample on the filter was transferred to a dialysis cassette

(MWCO 2000 Da) and dialyzed against distilled water. The micelle solutions were lyophilized and stored at -20°C until use.

Determination of % reaction and degree of porphyrin conjugation with PMC: To quantify the amount of unreacted porphyrin amine, the absorbance at 425 nm of the first filtrate collected after ultrafiltration was measured by UV-Vis (Nanodrop, Pedestal mode). From a standard curve of porphyrin in water (Figure S3), the concentration of porphyrin amine in the filtrates of the PMC1, 2 and 3 reaction mixtures were quantified.

From these values, the % reaction as well as the degree of conjugation (number of porphyrin groups per PAM-PPFPA polymer) were calculated for PMC1, 2 and 3 using the following equations:

% Reaction = 
$$(1 - \frac{[Porphyrin in filtrate]}{[Porphyrin in feed]}) \times 100$$
 (1)

% Reaction = 
$$(1 - \frac{[Porphyrin in filtrate]}{[Porphyrin in feed]}) \times 100$$
 (1)  
Degree of conjugation =  $(\frac{[porphyrin]_{Feed}}{[PFPA]}) \times 26 \times \frac{\% Reaction}{100}$  (2)

Mn complexation of porphyrin amine: Aqueous solutions of porphyrin amine and Mn(OAc)2 were mixed at a final porphyrin amine concentrations of 40 µM and Mn/porphyrin molar ratios ranging from 0.5-200. After keeping the solutions at 40°C for 1 d, the UV-Vis spectra were measured by Nanodrop (pedestal mode) (Figure S4). With the increase of Mn(OAc)<sub>2</sub> concentration, the peak at 425 nm of porphyrin amine decreased and the peak at 464 nm corresponding to the Mn/porphyrin amine complex increased showing an isosbestic point at 450 nm. % Mn complexation was calculated using the following equation:

$$\% Mn complexation = \frac{\left[\frac{\triangle Abs_{464}}{Abs_{450}}\right]}{2.4} \times 100 \tag{3}$$

Where  $Abs_{450}$  is the absorbance at 450 nm and  $\Delta Abs_{464}$  the change in absorbance at 464 nm upon complexation at the specified Mn/porphyrin molar ratio.

Complexation of porphyrin-modified micelles (PMC) with Mn(OAc)<sub>2</sub> (MnPMC): Lyophilized PMC were resuspended in water at 5 mg/mL and porphyrin concentration was determined by UV-Vis by measuring the absorbance at 425 nm. The PMC solutions were mixed with aqueous Mn(OAc)<sub>2</sub> solutions giving Mn/porphyrin molar ratios of 5-200, and incubated at 40°C for 1 d. Extent of manganese complexation was determined by measuring UV-Vis spectra as shown in **Figure S5**. All PMC showed a plateau with a maximum complexation of 93% (PMC 1), 91% (PMC 2) and 76% (PMC 3) at Mn/porphyrin molor ratios of 10,50 and 100 respectively. The micelle solutions were dialyzed against distilled water (MWCO 2000 Da) and stored at -20°C until use. The concentration of Mn-porphyrin in the micelle solution was determined by measuring the absorbance at 464 nm.

Stability of the Mn-porphyrin amine complex and MnPMCs in 10% Fetal Bovine serum (FBS): A solution containing porphyrin amine (60 μM) and Mn(OAc)<sub>2</sub> (3 mM, 50 eq) in distilled water was incubated at 40°C for 1 d. To 50 μL of this solution, 50 μL of FBS and 400 μL 10X D-PBS were added resulting in a final concentration of 10% FBS. The solution was kept for 2 d at 37°C and transferred to a quartz cuvette to measure the UV-Vis spectra (Figure 3a).

To 10 μL of MnPMC solutions (Mn/porphyrin concentrations: 33 (MnPMC1), 58 (MnPMC2) and 61 μM (MnPMC1)) were added 2 μL FBS, 2 μL 10X D-PBS and 6 μL water. The solutions were incubated for 2 d at 37°C and measured by UV-Vis using Nanodrop (pedestal mode) (**Figure 3b-d**).

MnPMC2-catalyzed formation of polysulfide detection using the SSP4 detection dye: MnPMC2 and PMC2 solutions at 2  $\mu$ M were prepared by diluting stock solutions in water with 10X PBS. As a control PBS was used. To 500  $\mu$ L Qubit assay tubes were added 200  $\mu$ L

MnPMC2, PMC2 and PBS, followed by 2  $\mu$ L SSP4 (1 mM in DMSO) and 20  $\mu$ L of a freshly prepared solution of Na<sub>2</sub>S (1 mM) in water. After adding Na<sub>2</sub>S, the tubes were closed immediately to avoid evaporation of H<sub>2</sub>S. There was sufficient headspace to make sure that enough oxygen was available for the oxidation reaction. The green fluorescence intensity was measured in the Qbit 4 fluorometer (Excitation: Blue LED, 430-490 nm, Emission: 510-580 nm) and the samples were placed at 37°C. At the indicated time, the fluorescence intensity was measured.

Preparation of glutathione polysulfide adducts of TME-IAM with Na<sub>2</sub>S<sub>2</sub>: The glutathione (GSH) and glutathione persulfide (GS-(S)<sub>n</sub>-H, n=1 or 2 ) adducts with TME-IAM were synthesized as reported but using Na<sub>2</sub>S<sub>2</sub> instead of Na<sub>2</sub>S<sub>3</sub>.<sup>[4]</sup> In a 1.5 mL Eppendorf tube, a solution containing 0.5 mM GSH and 0.5 mM Na<sub>2</sub>S<sub>2</sub> in 10 mM Tris-HCl buffer (pH 7.4) was reacted at room temperature in the dark for 30 min. Then, a solution of TME-IAM (100 mM) in DMSO was added to a final concentration of 5 mM. After reacting at 37°C for 1 h, the mixtures were stored at -20°C until analysis by HPLC/MS-MS.

MnPMC2-catalyzed formation of glutathione polysulfide adducts by HPLC-MS/MS: In 1.5 mL tubes, aqueous solutions of MnPMC2, PMC2 and water were sequentially mixed with glutathione and Na<sub>2</sub>S in 10 mM Tris buffer at pH 7.4. (Total volume: 200 μL. Final concentrations: MnPMC 2 and PMC 2: 100 μM, glutathione: 500 μM, Na<sub>2</sub>S: 1 mM) After adding Na<sub>2</sub>S, the tubes were closed immediately to avoid evaporation of H<sub>2</sub>S. There was sufficient headspace to make sure that enough oxygen was available for the oxidation reaction. Then, the mixture was incubated at 37°C in the dark. After 1 h, the additional 4 μL of a 50 mM Na<sub>2</sub>S/water was added. After 1 h of incubation at 37°C, 10 μL of a 100 mM TME-IAM solution was added to the solutions and reacted at 37°C for 1 h. The solutions were

then transferred to an Amicon ultrafiltration system (MWCO 30kDa) and centrifuged at 14,000 g for 10 min. The filtrate was collected and stored at -20°C until HPLC-MS/MS analysis.

Fluorescence detection of intracellular persulfide species in HUVECs: Four-well glass-bottom dishes were coated with 100  $\mu$ L/well of 2% Matrigel for 30 min at 37°C. After aspirating excess solution, HUVECs were seeded at 5 x 10³ cells/well and cultured for 2 d. The culture medium was replaced with 100  $\mu$ L/well fresh culture medium (phenol red free) containing 25  $\mu$ M SSP4 dye and cultured for 1 h. After washing the cells with culture medium, 100  $\mu$ L/well fresh culture medium (phenol red free) containing MnPMC2 (Mnporphyrin concentration: 2  $\mu$ M), and/or ADT (100  $\mu$ M) was added. Cells were cultured for 1.5 h, stained with Hoechst 33342 (0.125  $\mu$ g/mL in culture medium) for 15 min and observed by confocal laser scanning fluorescence microscopy (CLSFM).

Tube formation assay: The fibrinogen solution in PBS (5 mg/mL) was mixed with thrombin (final concentration: 1 U/mL) and immediately added to an Ibidi μ-slide (10 μL/well). The slide was incubated at 37°C for 30 min. To each well, 30 μL/well of medium containing MnPMC2 (5.8 μM) and/or ADT (10 μM) was added. HUVECs were suspended in culture medium at 4 x 10<sup>5</sup> cells/mL and added to the slide at 25 μL/well. After culturing the cells for 2 d, Phase contrast images were acquired to determine the number of loops per well (**Figure S7**). The culture medium was replaced with 4% PFA/PBS. The slide was kept at room temperature for 20 min and washed with PBS. After fixation, cells were permeabilized with 0.2% Triton X-100 for 15 min, washed with PBS twice and treated with reagent diluent (BSA solution) for 1.5 h. After removing reagent diluent, cells were stained with Fluorescein-Phalloidin (1:400 dilution with Reagent Diluent) for 1 h, washed with PBS three times, and

stained with Hoechst 33342 (5  $\mu$ g/mL in PBS) for 10 min. The fluorescence images were collected by CLSFM.

Morphological analysis of HUVECs: Four-well glass-bottom dish was treated with 10% Matrigel for 30 min at 37°C. The residual solution was aspirated. HUVECs were seeded at 2 x 10<sup>4</sup> cells/well and cultured for 2 d. The culture medium was replaced with 100 μL/well of fresh culture medium (phenol-red free) containing MnPMC 2 (5.8 μM Mn-porphyrin), and /or ADT (10 μM) was added. Cells were cultured for 1 d, fixed with 4% PFA/PBS for 15 min and washed with PBS. Cells were permeabilized with 0.2% Triton X-100/PBS for 15 min and blocking with 1% BSA/PBS (Reagent Diluent) for 1.5 h. Actin filaments were stained with fluorescein-phalloidin (1:400 dilution with Reagent Diluent) for 1 h. VE-cadherin was stained with mouse anti-human VE-cadherin antibody (1:50 dilution with Reagent Diluent) for 1 h and thereafter Alexafluor 488-labeled goat anti-mouse IgG (1:200 dilution with Reagent Diluent) for 1 h. Nuclei were stained with Hoechst 33324 (5 μg/mL in PBS) for 10 min. For each step, the samples were washed with PBS three times. The fluorescence images were collected by CLSFM.

The image analysis was performed as outlined in **Figure S11**. The outer edges of cells were drawn manually using ImageJ software and Photoshop software. The extracted outer edge images were used to identify cell shape. To analyze cell elongation and alignment, the ellipse approximation of cell shape was performed using Fiji software. The elongation factor for each cell was calculated by dividing the major axis over the minor axis (**Figure S9**). The angle of cell main axis (major axis of ellipse) was determined for each cell in a confocal image (3 images per group) and the deviation from the average angle was calculated by subtracting the average cell angle for each image from angle of each cell (**Figure S10**).

Statistical Analysis: Data are expressed as mean  $\pm$  SD. The sample size was n=3 for all cell experiments. The statistical significance of the experimental data was analyzed with a two-tailed Student t-test using Microsoft Excel software. In all cases, significance was defined as \*p<0.05.

#### **Supporting Information**

Supporting Information is available from the Wiley Online Library or from the author.

#### Acknowledgements

This work was supported by the U.S. National Science Foundation (NSF), CBET, 2102848. S.Y. acknowledges financial support from the National Institute of Technology Faculty Research Abroad Program, Japan. The authors acknowledge the Huck Metabolomics Core Facility, Penn State, for use of the Sciex TripleTOF 5600 system and Dr. Sergei Koshkin for collecting the HPLC-MS/MS data.

Received: ((will be filled in by the editorial staff))

Revised: ((will be filled in by the editorial staff))

Published online: ((will be filled in by the editorial staff))

#### References

- [1] K. Abe, H. Kimura, *The Journal of Neuroscience* **1996**, *16*, 1066-1071.
- B. L. Predmore, K. Kondo, S. Bhushan, M. A. Zlatopolsky, A. L. King, J. P. Aragon,
   D. B. Grinsfelder, M. E. Condit, D. J. Lefer, *American Journal of Physiology Heart and Circulatory Physiology* 2012, 302, H2410-H2418.
- [3] L.-F. Hu, M. Lu, C. X. Tiong, G. S. Dawe, G. Hu, J.-S. Bian, *Aging Cell* **2010**, *9*, 135-146.
- [4] M. Ferlito, Q. Wang, W. B. Fulton, P. M. Colombani, L. Marchionni, K. Fox-Talbot, N. Paolocci, C. Steenbergen, *The Journal of Immunology* **2014**, *192*, 1806-1814.

- [5] Z. W. Lee, X. Y. Teo, E. Y. W. Tay, C. H. Tan, T. Hagen, P. K. Moore, L. W. Deng, *British Journal of Pharmacology* **2014**, *171*, 4322-4336.
- [6] M. Iciek, A. Bilska-Wilkosz, M. Kozdrowicki, M. Górny, *Bioscience Reports* **2022**, 42.
- [7] M. R. Filipovic, J. Zivanovic, B. Alvarez, R. Banerjee, *Chemical Reviews* **2018**, *118*, 1253-1337.
- [8] A. K. Mustafa, M. M. Gadalla, N. Sen, S. Kim, W. Mu, S. K. Gazi, R. K. Barrow, G. Yang, R. Wang, S. H. Snyder, *Science Signaling* **2009**, *2*, ra72-ra72.
- [9] J. Kang, A. J. Ferrell, W. Chen, D. Wang, M. Xian, *Organic Letters* 2018, 20, 852-855.
- [10] B. Yu, Y. Zheng, Z. Yuan, S. Li, H. Zhu, L. K. De La Cruz, J. Zhang, K. Ji, S. Wang, B. Wang, *Journal of the American Chemical Society* **2018**, *140*, 30-33.
- [11] a) K. M. Dillon, H. A. Morrison, C. R. Powell, R. J. Carrazzone, V. M. Ringel-Scaia, E. W. Winckler, R. M. Council-Troche, I. C. Allen, J. B. Matson, *Angewandte Chemie International Edition* **2021**, *60*, 6061-6067; b) C. R. Powell, K. M. Dillon, Y. Wang, R. J. Carrazzone, J. B. Matson, *Angewandte Chemie International Edition* **2018**, *57*, 6324-6328; c) K. M. Dillon, R. J. Carrazzone, Y. Wang, C. R. Powell, J. B. Matson, *ACS Macro Letters* **2020**, *9*, 606-612.
- [12] K. G. Fosnacht, M. M. Cerda, E. J. Mullen, H. C. Pigg, M. D. Pluth, *ACS Chemical Biology* **2022**, *17*, 331-339.
- [13] a) K. R. Olson, Y. Gao, F. Arif, S. Patel, X. Yuan, V. Mannam, S. Howard, I. Batinic-Haberle, J. Fukuto, M. Minnion, M. Feelisch, K. D. Straub, *Antioxidants* **2019**, *8*, 639; b) K. R. Olson, Y. Gao, F. Arif, K. Arora, S. Patel, E. R. DeLeon, T. R. Sutton, M. Feelisch, M. M. Cortese-Krott, K. D. Straub, *Redox Biology* **2018**, *15*, 74-85.

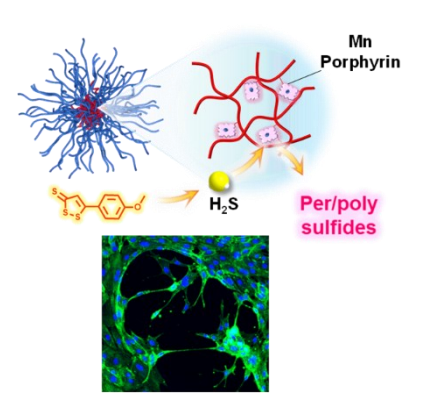
- [14] T. Bostelaar, V. Vitvitsky, J. Kumutima, B. E. Lewis, P. K. Yadav, T. C. Brunold, M. Filipovic, N. Lehnert, T. L. Stemmler, R. Banerjee, *Journal of the American Chemical Society* **2016**, *138*, 8476-8488.
- [15] a) P. Rose, B. W. Dymock, P. K. Moore, *Methods Enzymol* 2015, 554, 143-167; b) R. J. Carrazzone, J. C. Foster, Z. Li, J. B. Matson, *European Polymer Journal* 2020, 141, 110077; c) C. R. Powell, J. C. Foster, B. Okyere, M. H. Theus, J. B. Matson, *Journal of the American Chemical Society* 2016, 138, 13477-13480; d) C. R. Powell, K. Kaur, K. M. Dillon, M. Zhou, M. Alaboalirat, J. B. Matson, *ACS Chemical Biology* 2019, 14, 1129-1134; e) J. J. Y. Chen, A. J. van der Vlies, U. Hasegawa, *Polymer Chemistry* 2020, 11, 4454-4463; f) U. Hasegawa, A. J. van der Vlies, *Bioconjugate Chemistry* 2014, 25, 1290-1300; g) U. Hasegawa, A. J. van der Vlies, *MedChemComm* 2015, 6, 273-276; h) A. J. van der Vlies, M. Ghasemi, B. M. Adair, J. H. Adair, E. D. Gomez, U. Hasegawa, *Adv Healthc Mater* 2023, 12, e2201836; i) M.-M. Dali, P. M. Dansette, D. Mansuy, J.-L. Boucher, *Drug Metabolism and Disposition* 2020, 48, 426-431; j) A. Martelli, L. Testai, V. Citi, A. Marino, I. Pugliesi, E. Barresi, G. Nesi, S. Rapposelli, S. Taliani, F. Da Settimo, M. C. Breschi, V. Calderone, *ACS Med Chem Lett* 2013, 4, 904-908; k) Y. Zhao, M. D. Pluth, *Angewandte Chemie International Edition* 2016, 55, 14638-14642.
- [16] A. J. van der Vlies, J. Xu, M. Ghasemi, C. Bator, A. Bell, B. Rosoff-Verbit, B. Liu, E.D. Gomez, U. Hasegawa, *Biomacromolecules* 2022, 23, 77-88.
- [17] S. Asayama, K. Mizushima, S. Nagaoka, H. Kawakami, *Bioconjugate Chemistry* **2004**, *15*, 1360-1363.
- [18] I. Yakavets, I. Yankovsky, L. Bezdetnaya, V. Zorin, *Dyes and Pigments* **2017**, *137*, 299-306.
- [19] L. Li, M. Whiteman, Y. Y. Guan, K. L. Neo, Y. Cheng, S. W. Lee, Y. Zhao, R. Baskar, C. H. Tan, P. K. Moore, *Circulation* **2008**, *117*.

- [20] M. Shieh, X. Ni, S. Xu, S. P. Lindahl, M. Yang, T. Matsunaga, R. Flaumenhaft, T. Akaike, M. Xian, *Redox Biology* **2022**, *56*, 102433.
- [21] S. Kasamatsu, T. Ida, T. Koga, K. Asada, H. Motohashi, H. Ihara, T. Akaike, *Antioxid Redox Signal* **2021**, *34*, 1407-1419.
- [22] a) A. Papapetropoulos, A. Pyriochou, Z. Altaany, G. Yang, A. Marazioti, Z. Zhou, M. G. Jeschke, L. K. Branski, D. N. Herndon, R. Wang, C. Szabó, *Proceedings of the National Academy of Sciences* **2009**, *106*, 21972-21977; b) S.-I. Bibli, J. Hu, M. Looso, A. Weigert, C. Ratiu, J. Wittig, M. K. Drekolia, L. Tombor, V. Randriamboavonjy, M. S. Leisegang, P. Goymann, F. D. Lagos, B. Fisslthaler, S. Zukunft, A. Kyselova, A. F. O. Justo, J. Heidler, D. Tsilimigras, R. P. Brandes, S. Dimmeler, A. Papapetropoulos, S. Knapp, S. Offermanns, I. Wittig, S. L. Nishimura, F. Sigala, I. Fleming, *Circulation* **2021**, *143*, 935-948.
- [23] D. Zhang, J. Du, C. Tang, Y. Huang, H. Jin, Front Pharmacol 2017, 8, 608.
- [24] a) B. Umaru, A. Pyriochou, V. Kotsikoris, A. Papapetropoulos, S. Topouzis, *J Pharmacol Exp Ther* **2015**, *354*, 79-87; b) G. Meng, S. Zhao, L. Xie, Y. Han, Y. Ji, *Br J Pharmacol* **2018**, *175*, 1146-1156.
- [25] J. Cao, M. Ehling, S. März, J. Seebach, K. Tarbashevich, T. Sixta, M. E. Pitulescu, A.C. Werner, B. Flach, E. Montanez, E. Raz, R. H. Adams, H. Schnittler, *Nature Communications* 2017, 8, 2210.
- [26] T. L. Bach, C. Barsigian, D. G. Chalupowicz, D. Busler, C. H. Yaen, D. S. Grant, J. Martinez, *Exp Cell Res* **1998**, *238*, 324-334.
- [27] A.-C. Vion, T. Perovic, C. Petit, I. Hollfinger, E. Bartels-Klein, E. Frampton, E. Gordon, L. Claesson-Welsh, H. Gerhardt, *Frontiers in Physiology* **2021**, *11*.
- [28] L. Lamalice, F. L. Boeuf, J. Huot, Circulation Research 2007, 100, 782-794.
- [29] S. Yuan, S. Pardue, X. Shen, J. S. Alexander, A. W. Orr, C. G. Kevil, *Redox Biology* **2016**, *9*, 157-166.

Manganese porphyrin-containing polymeric micelles (MnPMCs) catalyze oxidization of hydrogen sulfide (H<sub>2</sub>S) to per/polysulfide species. Co-delivery of the H<sub>2</sub>S donor anethole dithiolethione and MnPMCs increases intracellular per/polysulfide levels and induces proangiogenic response in human umbilical vein endothelial cells.

K. Young, S. Yamane, E. A. Ghareh Tapeh, S. Kasamatsu, H. Ihara, U. Hasegawa\*

Manganese porphyrin-containing polymeric micelles: A novel approach for intracellular catalytic formation of per/polysulfide species from a hydrogen sulfide donor ToC figure



### **Supporting Information**

Manganese porphyrin-containing polymeric micelles: A novel approach for intracellular catalytic formation of per/polysulfide species from a hydrogen sulfide donor

Kemper Young, Setsuko Yamane, Elmira Abbasi GharehTapeh, Shingo Kasamatsu, Hideshi Ihara, Urara Hasegawa\*

#### Instrumentation

<sup>1</sup>H NMR: <sup>1</sup>H NMR spectra of the polymers were measured in deuterated chloroform (CDCl<sub>3</sub>) on a Bruker NEO-400 instrument. A total of 32 scans were collected and the D1 was set to 10 seconds. The chemical shifts are reported relative to the residual CHCl<sub>3</sub> signal at 7.26 ppm. Measured spectra were processed with the TopSpin 4.0.7 software.

Size exclusion chromatography combined with multiangle laser light scattering (SEC-MALLS): Elution profiles of the polymers were obtained on a Waters Alliance e2695 HPLC system equipped with a 2414 refractive index (RI) detector and a Wyatt DAWN 8 multiangle light scattering detector. A ResiPore PL1113-6300 column and a ResiPore PL1113-1300 guard column were used Agilent (USA). THF (HPLC grade) was used as the eluent at a flow rate of 1.0 mL/min. The temperature of the column oven and the RI detector was 40 °C. The dn/dc values were estimated by assuming 100% mass recovery. The Mw and Mn values of the polymer were determined by Zimm plot using a refractive index increment (dn/dc) value of 0.1247 was calculated using the equation (S1), where wi is the weight fraction and (dn/dc)i refractive index increment of the homopolymers: 0.052 for PAM and 0.155 for PPFPA.

$$\frac{dn}{dc} = w_{PPFPA} \left(\frac{dn}{dc}\right)_{PPFPA} + w_{PAM} \left(\frac{dn}{dc}\right)_{PAM} \tag{S1}$$

Dynamic light scattering (DLS): Hydrodynamic diameters of the micelles were obtained a Malvern Zetasizer Nano ZS Series instrument and disposable micro cuvettes (ZEN0040, Malvern). The Z-average diameter and polydispersity index were determined by the cumulant method.

*Transmission electron microscopy (TEM)*: A solution of the micelles in water (Porphyrin concentration: 2 μM) was placed onto a Formvar/caron-coated 400 mesh copper grid (Tedd Pella) and then dried by blotting the side of the grid with filter paper. Then, the grid was negatively stained with 2 wt% uranyl acetate solution. The TEM imaging was done using a ThermoFisher Scientific Tecnai G2 TEM at 200 kV.

*UV-Vis spectroscopy*: Spectra were obtained on a Thermo Scientific Nanodrop One<sup>c</sup> instrument.

Fluorescence measurement: Fluorescence intensities were measured with a Qubit 4 fluorometer (ThermoFisher Scientific) in 50 μL polypropylene Eppendorf tubes. Excitation wavelengths: 430-495 nm and emission wavelengths: 510-580 nm.

HPLC-MS/MS: Samples were analyzed by a Shimadzu Prominence UFLC system coupled with an Sciex TripleTOF 5600 QqTOF mass spectrometer equipped with a Duo-Spray ion source. For analysis, the samples components were separated by using a Waters (Milford, MA) CSH C18 column (2.1 × 150 mm, 1.7 μm particle size). The column temperature was 40 °C. The solvent A of the mobile phase was LC-MS grade water containing 0.1 % formic acid and solvent B of the mobile phase was LC-MS grade acetonitrile containing 0.1 % formic acid. The flow rate of the mobile phase was 0.300 mL/min. The gradient of solvent B was 0-2.0 min 2% of B, 6.0 min 85% of B, 10.0 min 100% of B, 10.5 min 2% of B and 10.5-15.0 min 2% (B). The analysis was carried out in the positive ion detection mode. During the

analysis, an ion spray voltage (IS) of 5500 V, curtain gas (CUR) of 30 psi, nebulizer gas (GS1) of 60 psi, heater gas 2 (GS2) of 50, and heater temperature (TEM) of 550 C were applied. The MS1 data collection was conducted with a scan range from 100 to 1200 m/z for full scan. Fragmentation data were collected using the data dependent MS2 data acquisition mode with collision energy of 35 eV and collision energy spread 15 eV.

Confocal laser scanning fluorescence microscopy (CLSFM): Fluorescent images were acquired on an Olympus FluoView FV1000-D confocal laser scanning fluorescence microscope equipped with 405, 473, 559 and 635 nm lasers.

Phase contrast microscopy: an EVOS phase contrast microscope with a 4x objective lens was used.

#### Materials

4-acryloylmorpholine (AM), acryloyl chloride, 2,2'-azobis(isobutyronitrile) (AIBN), 2-(dodecylthiocarbonothioylthio)-2-methylpropionic acid (CTA), aluminum oxide (Al<sub>2</sub>O<sub>3</sub>), deuterated chloroform (CDCl<sub>3</sub>), calcium hydride (CaH<sub>2</sub>), and 4Å molecular sieves, Tris·HCl, Na<sub>2</sub>S·9H<sub>2</sub>O were purchased from Sigma Aldrich (USA). 1,4-dioxane, anhydrous dimethylformamide (DMF), tetrahydrofuran (THF), diethyl ether (Et<sub>2</sub>O), ethanol (EtOH), triethylamine (TEA), potassium hydroxide (KOH), glutathione (reduced) were purchased from Fisher Scientific (USA). Tris(trimethylsilyl)silane was purchased from TCI. Na<sub>2</sub>S<sub>2</sub> was purchased from Dojindo. XPell pellets were purchased from Xplosafe (USA). Dialysis cassettes (MWCO 2 kDa) were purchased from Spectrum Laboratories (USA).

AIBN was recrystallized from MeOH and stored at -20°C until use. AM was passed through a plug of Al<sub>2</sub>O<sub>3</sub> to remove inhibitor. 1,4-dioxane was distilled from CaH<sub>2</sub> and kept over molecular sieves and XPell pellets. TEA was dried over KOH pellets before use.

Pentafluorophenyl acrylate (PFPA)<sup>[1]</sup>, porphyrin amine<sup>[2]</sup> and TME-IAM<sup>[3]</sup> were synthesized

as reported. The porphyrin amine HCl salt was converted to the free amine by reacting with excess TEA in DMF and precipitating in Et<sub>2</sub>O. The fine brown powder consisting of porphyrin amine and 4 TEA·HCl was dried under vacuum. The amount of porphyrin amine used for conjugation was corrected for the presence of the TEA·HCl salt. All other reagents were used as received without further purification.

Medium 200 and Low Serum Growth Supplement, 0.25% trypsin-EDTA (1X), trypsin neutralizer solution, Dulbecco's phosphate buffered saline (PBS), fetal bovine serum (FBS) and penicillin-streptomycin (P/S) (10,000 units/mL of penicillin and 10,000 μg/mL of streptomycin) and phosphate buffered saline (10X) were purchased from Gibco. Human umbilical vein endothelial cells (HUVEC, pooled donor) and Growth factor reduced Matrigel matrix was purchased from Corning. Vascular cell basal medium and endothelial cell growth kit were purchased from ATCC. Reagent Diluent (10X) was purchased from R&D systems. μ slide angiogenesis slides were purchased from Ibidi. Fibrinogen and thrombin (100 U/mL) were purchased from Sigma. 16% w/v methanol-free paraformaldehyde (PFA) solution, Hoechst 33342, Alexafluor 488-labeled goat anti-mouse IgG and Fluorescein-Phalloidin were purchased from Invitrogen. Mouse anti-human VE-cadherin antibody was purchased from EMD Millipore. SSP4 was purchased from Dojindo. ADT was purchased from ArkPharm. Triton X-100, Alexafluor 568-labeled goat anti-mouse IgG were purchased from Invitrogen.

Synthesis of poly(*N*-acryloyl morpholine)-*b*-poly(pentafluorophenyl acrylate) block copolymer (PAM-PPFPA).

The PAM-PPFPA polymer was synthesized as reported previously (**Scheme S1**).<sup>[4]</sup> PPFPA<sub>25</sub>-CTA polymer was synthesized by RAFT polymerization of PFPA. PFPA (916.4 mg, 3.85 mmol), CTA (56.3 mg, 0.154 mmol), and AIBN (2.5 mg, 0.0154 mmol) were dissolved in

1,4-dioxane (Total volume: 3.8 mL). The solution was deoxygenated by five freeze-pump-thaw cycles under an inert atmosphere of argon and placed in an oil bath at 60°C. After 24 h, the reaction was stopped by cooling in liquid nitrogen and exposing to air. The clear yellow solution was added dropwise to EtOH to precipitate the polymer. The polymer was collected by filtration, washed with EtOH and dried under reduced pressure.

PAM<sub>100</sub>-PPFPA<sub>25</sub>-CTA polymer was synthesized by RAFT polymerization of AM using PPFPA<sub>25</sub>-CTA polymer as the macro CTA. AM (282.3 mg, 2 mmol), PPFPA-CTA (126.3 mg, 0.02 mmol) and AIBN (0.328 mg, 0.002 mmol) were dissolved in 1,4-dioxane (Total volume: 2 mL). The solution was deoxygenated by five freeze-pump-thaw cycles under an inert atmosphere of argon and placed in an oil bath at 60°C. After 24 h, the reaction was stopped by cooling in liquid nitrogen and exposing to air. The clear yellow solution was added dropwise to Et<sub>2</sub>O to precipitate the polymer. The polymer was collected by filtration, washed with Et<sub>2</sub>O and dried under reduced pressure.

The CTA end group was removed by radical-induced reduction. PAM<sub>100</sub>-PPFPA<sub>25</sub>-CTA polymer (225 mg, 0.0110 mmol), tris(trimethylsilyl)silane (13.7 mg, 0.0551 mmol) and AIBN (3.6 mg, 0.022 mmol) were dissolved in 1.5 mL of 1,4-dioxane. The solution was deoxygenated by five freeze-pump-thaw cycles under an inert atmosphere of argon and placed in an oil bath at 70°C. After 24 h, the reaction was stopped by cooling in liquid nitrogen and exposing to air. The colorless solution was added dropwise to Et<sub>2</sub>O to precipitate the polymer. The polymer was collected by filtration, washed with Et<sub>2</sub>O and dried under reduced pressure. The polymers were characterized by  $^{1}$ H NMR (**Figures S1**) and SEC-MALLS (**Figures S2**). The degrees of polymerization,  $M_{w}$ ,  $M_{n}$  and  $M_{w}/M_{n}$  of PPFPA<sub>25</sub>-CTA, PAM100-PPFPA<sub>25</sub>-CTA and PAM<sub>100</sub>-PPFPA<sub>25</sub> are summarized in **Table S1**.

#### Fluorine NMR spectroscopy

MnPMC 2 were lyophilized and redispersed in CDCl<sub>3</sub> (2 mg/mL). PAM-PPFPA polymer (2 mg/mL in CDCl<sub>3</sub>) was also measured as a control. It should be noted that PAM-PPFPA polymer was stored under humid air (without replacing air with inert gas) for more than one year, and therefore PFPA group was partially hydrolyzed. <sup>19</sup>F NMR spectra in CDCl<sub>3</sub> were measured with a Bruker Bruker NEO-400 spectrometer. A number of 64 scans was collected and the delay time (D1) was set to 1 s. The chemical shifts are referenced against CF<sub>3</sub>COOH at -76.55 ppm. As shown in **Figure S6**, the peaks due to PFPA group bound to the polymer as well as pentafluorophenol (hydrolysis product) were observed. On the other hand, no peak was observed for MnPMC. The result clearly shows that the absence of PFPA group as well as hydrolysis product of PFPA group (pentafluorophenol) in MnPMCs.

#### Cell culture

HUVECs were cultured in Medium 200 supplemented with Low Serum Growth Supplement and 10 U/mL penicillin–10  $\mu$ g/mL streptomycin. Cells with passage number 4-6 were used for the experiments. Cells were cultured in phenol-red free vascular cell basal medium supplemented with endothelial cell growth kit (ATCC) for the confocal microscopy experiments.

#### Cell viability assay

HUVECs were seeded at  $2x10^4$  cells/well in a 96 well plate and cultured for 2 d. The culture medium was replaced with 100  $\mu$ L/well of fresh culture medium containing MnPMC 2 (6 and 8  $\mu$ M Mn-porphyrin). After cells were cultured for 1 d, the medium was replaced with 100  $\mu$ L/well of 0.5 mg/mL MTT in culture medium. Cells were cultured for 5 hours. The formed

formazan crystals were dissolved in 100  $\mu$ L/well of 100 mg/mL SDS/0.01 M HCl (aq). The absorbance at 570 nm was measured using a plate reader. The cell viability was expressed as a percentage of the absorbance of the nontreated cells.

**Scheme S1**. Synthesis of the PAM100-PPFPA25 diblock copolymer. (i) AIBN, dioxane, 60°C, (ii) AIBN, 60°C, (iii) tris(isopropyl)silane, AIBN, 70°C.

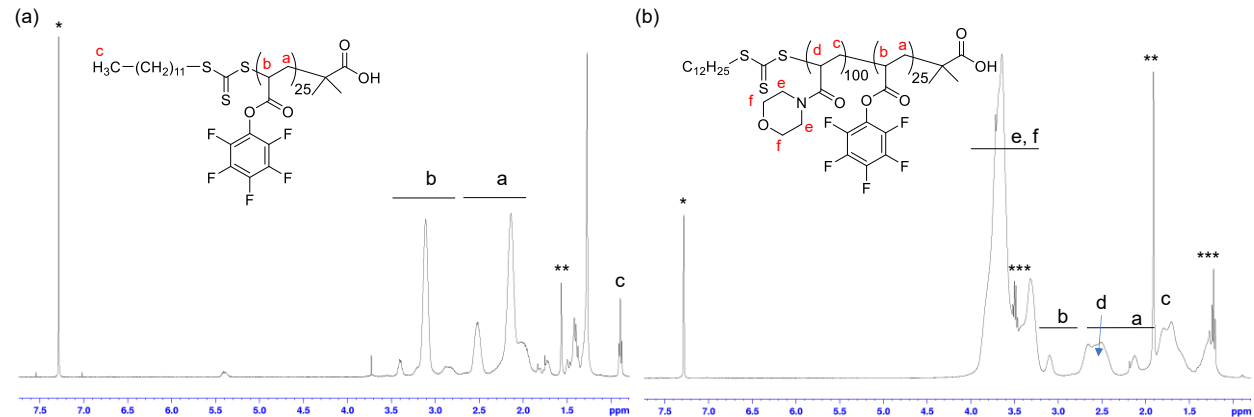
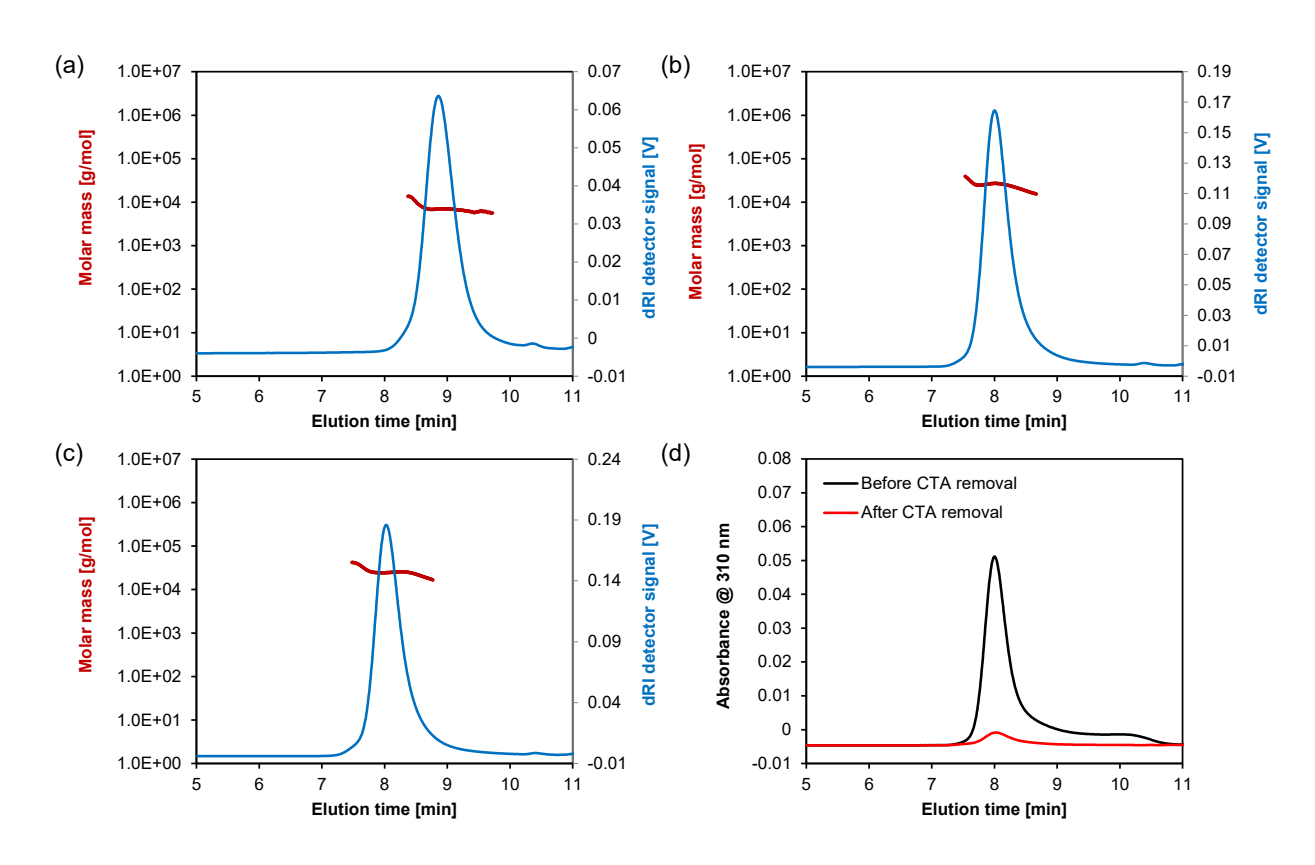


Figure S1. <sup>1</sup>H NMR spectra of (a) PPFPA-CTA and (b) PAM-PPFPA-CTA. Signals due to CHCl<sub>3</sub> (\*), water (\*\*), and diethyl ether (\*\*\*) have been marked.



**Figure S2.** SEC-MALLS elution profiles of (a) PPFPA-CTA and (b, d) PAM-PPFPA-CTA and (c,d) PAM-PPFPA (a-c) showing molar mass according to MALLS and RI signal (d) UV signal at 310 nm.

**Table S1.** The degrees of polymerization,  $M_w$ ,  $M_n$  and  $M_w/M_n$  of PPFPA25-CTA, PAM100-PPFPA25-CTA and PAM100-PPFPA25 according to <sup>1</sup>H NMR and SEC-MALLS.

	[Monomer] /[CTA]	M <sub>n</sub> [g/mol] (Theoritical)	Degree of polymerization (NMR)		M <sub>n</sub> [g/mol]	M <sub>n</sub> [g/mol]	M <sub>w</sub> [g/mol]	M <sub>w</sub> /M <sub>n</sub>
			PPFPA	PAM	(NMR)	(SEC-MALLS)	(SEC-MALLS)	(SEC-MALLS)
PPFPA-CTA	25	6317	25.8	-	6508	6965	7057	1.013
PAM-PPFPA-CTA	100	20434	25.8	92.3	19538	24760	25160	1.016
PAM-PPFPA	-	20157	-	-	-	24670	24900	1.009

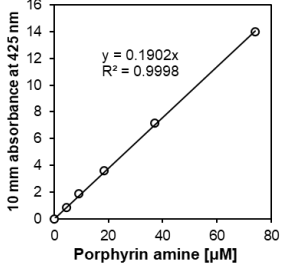


**Figure S3.** Porphyrin amine standard curve in water measured on a Nanodrop instrument (Pedestal mode).

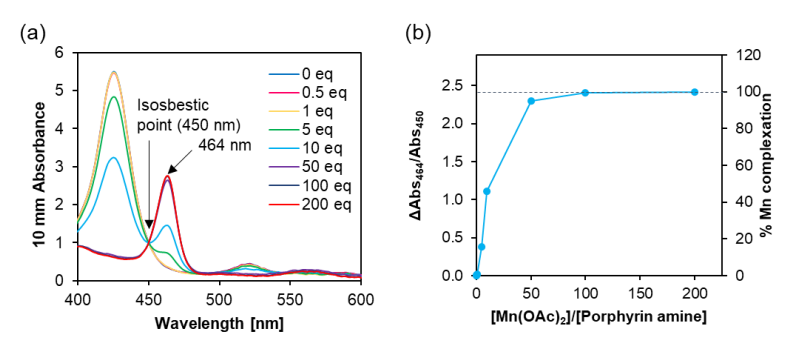


**Figure S4.** Effect of Mn(OAc)<sub>2</sub>/porphyrin amine molar ratio on the extent of manganese complexation by porphyrin. (a) UV-Vis spectra of aqueous solutions of porphyrin amine (concentration 40  $\mu$ M) with Mn(OAc)<sub>2</sub> at different molar ratios as measured on a Nanodrop instrument (Pedestal mode). (b) Plot of  $\Delta$ Abs<sub>464</sub>/Abs<sub>450</sub> and % Mn complexation calculated using equation (3) as function of the Mn(OAc)<sub>2</sub>/porphyrin amine molar ratios.

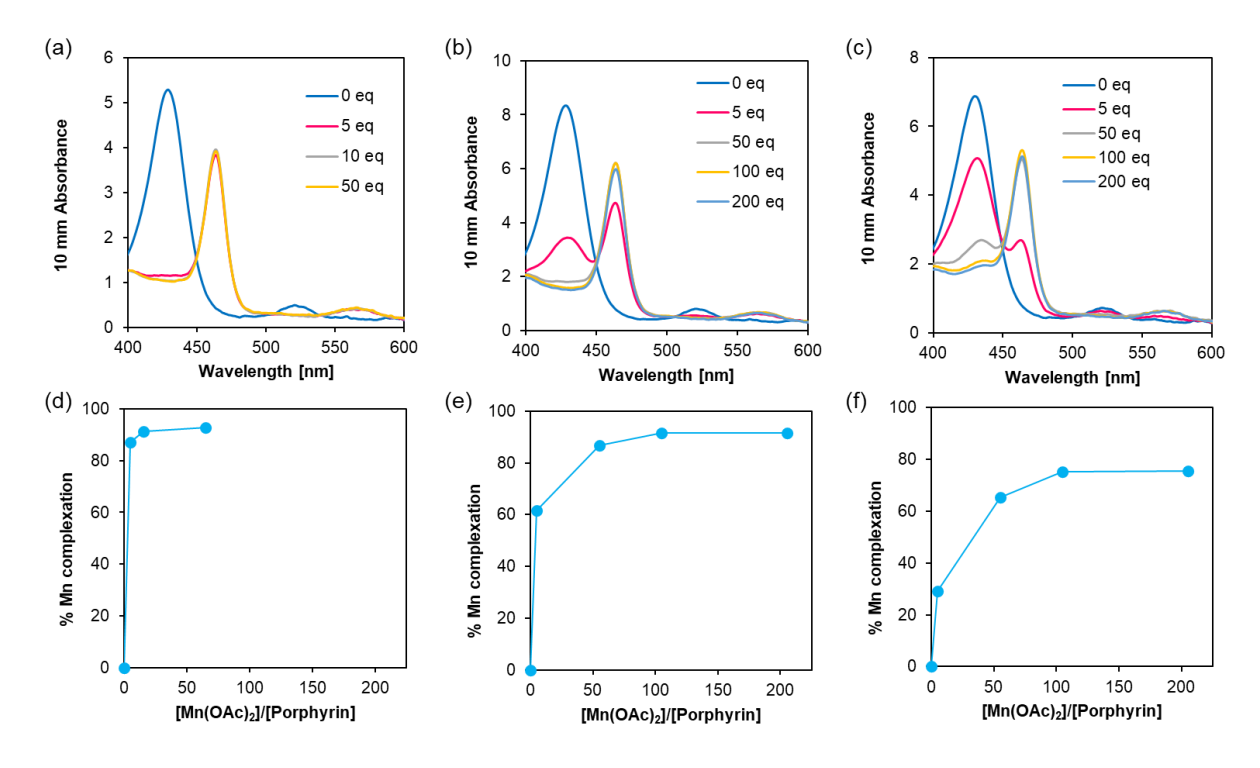


**Figure S5.** Complexation of PMCs with Mn(OAc)<sub>2</sub>. (a-c) UV-Vis spectra of aqueous solution before and after complexation with Mn(OAc)<sub>2</sub> as measured on a Nanodrop instrument (Pedestal mode) (d-f) Degree of Mn complexation calculated from the UV-Vis spectra using equation (3) as function of the Mn(OAc)<sub>2</sub>/porphyrin molar ratio. (a, d) PMC 1, (b, e) PMC 2, (c, f) PMC 3.

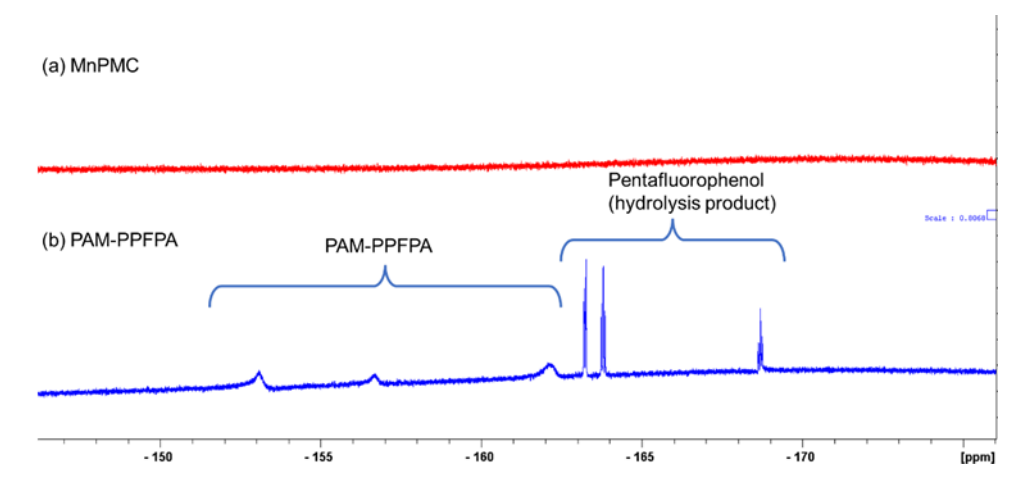


**Figure S6.** <sup>19</sup>F NMR of (a) MnPMCs and (b) partially hydrolyzed PAM-PPFPA. Solvent: CDCl<sub>3</sub>.

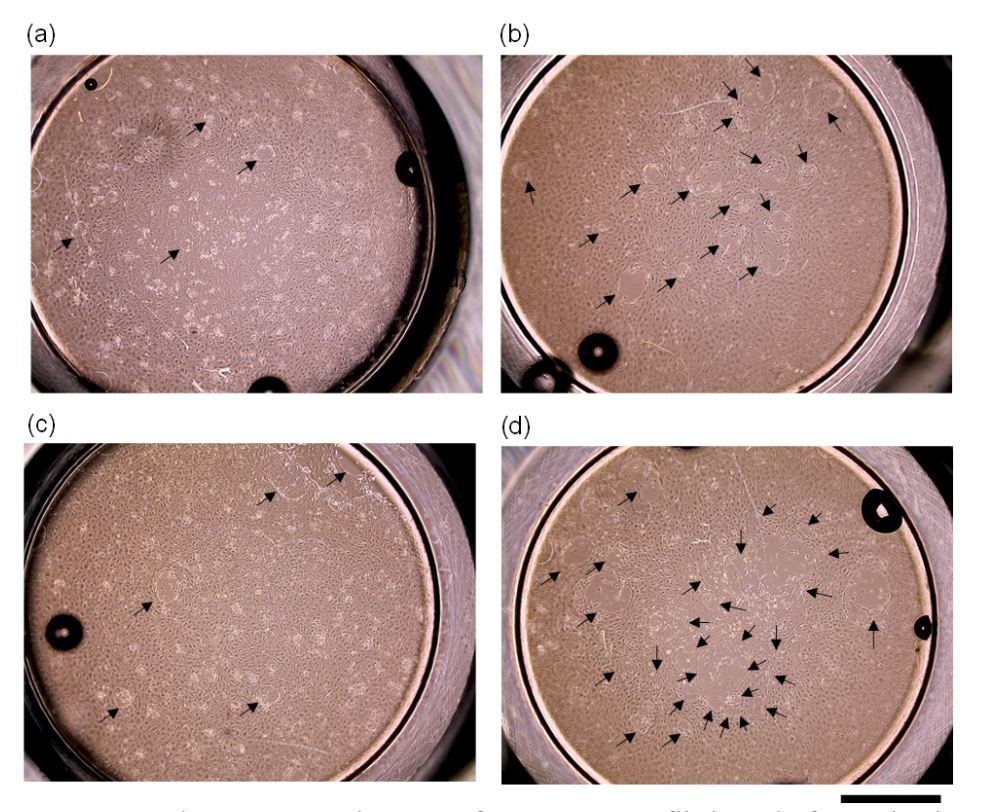


**Figure S7.** Phase contrast images of HUVECs on fibrin gel after culturing for 2 d.(a) NT, (b) ADT, (c) MnPMC, (d) MnPMC and ADT. Arrows indicate loops. Scale bar: 1 mm

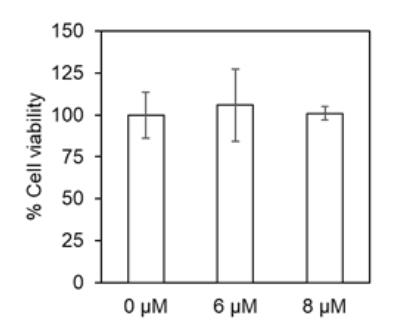


**Figure S8.** The effect of MnPMCs on viability of HUVECs. HUVECs were cultured in the presence of different concentrations of MnPMCs for 1 d and cell viability was determined by MTT assay. *n*=3.

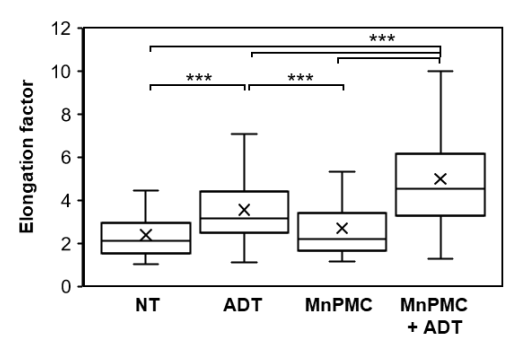


**Figure S9.** Cell elongation. Elongation factor determined from the confocal images of HUVECs in confluent culture. Cells were cultured in the presence of (a) medium alone, (b) ADT, (c) MnPMC2 and (d) MnPMC2 and ADT. MnPMC2: 5.8  $\mu$ M (Mn porphyrin), ADT 10  $\mu$ M. X: Mean. n=110-133. \*\*\*p<0.001.

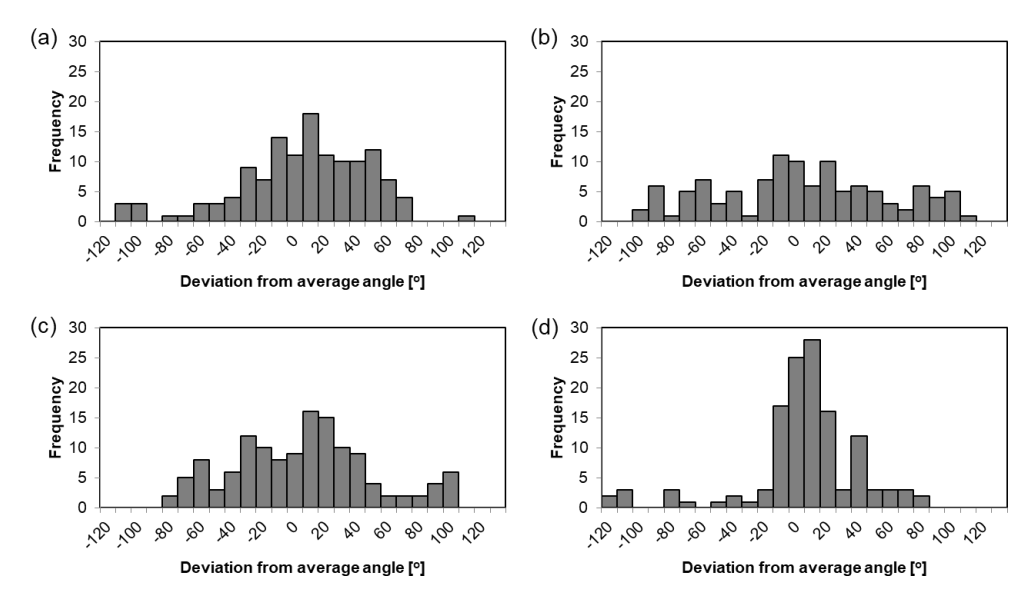


**Figure S10.** Cell alignment. Deviation from average angle of cell main axis was determined from the confocal images of HUVECs in confluent culture. Cells were cultured in the presence of (a) medium alone, (b) ADT, (c) MnPMC2 and (d) MnPMC2 and ADT. MnPMC2:  $5.8 \mu M$  (Mn porphyrin), ADT  $10 \mu M$ .

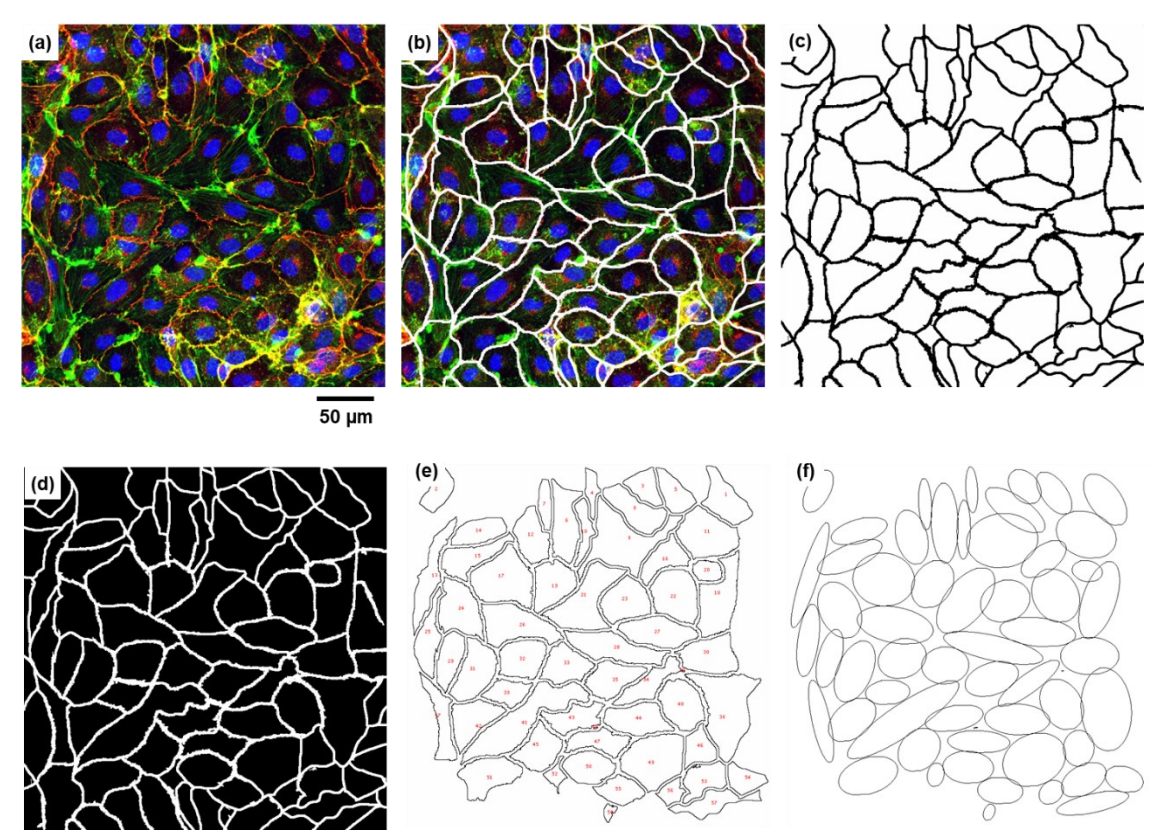


**Figure S11.** Elongation factor analysis. Image analysis. (a) Fluorescence image. (b) Drawing outer edge of cells. (c) outer edge of cells. (d) Inverted image of outer edge of cells. (e) Extracted cell shape. (f) Ellipse approximation.

#### **References:**

- [1] P. A. Woodfield, Y. Zhu, Y. Pei, P. J. Roth, Macromolecules 2014, 47, 750-762.
- [2] (a) S. Asayama, K. Mizushima, S. Nagaoka, H. Kawakami, Bioconjugate Chemistry 2004, 15, 1360-1363; (b) K. Kalyanasundaram, Inorganic Chemistry 1984, 23, 2453-2459.
- [3] S. Kasamatsu, T. Ida, T. Koga, K. Asada, H. Motohashi, H. Ihara, T. Akaike, Antioxid Redox Signal 2021, 34, 1407-1419.
- [4] A. J. van der Vlies, J. Xu, M. Ghasemi, C. Bator, A. Bell, B. Rosoff-Verbit, B. Liu, E. D. Gomez, U. Hasegawa, Biomacromolecules 2022, 23, 77-88.